Influence of Semicrystalline Homopolymer Addition on the Morphology of Semicrystalline Diblock Copolymers

Pratima Rangarajan,[†] Charles F. Haisch, and Richard A. Register*

Department of Chemical Engineering, Princeton University, Princeton, New Jersey 08544

Douglas H. Adamson[‡] and Lewis J. Fetters

Exxon Research and Engineering Company, Annandale, New Jersey 08801

Received February 26, 1996; Revised Manuscript Received October 30, 1996[⊗]

ABSTRACT: We have studied blends of polyethylene "homopolymer" (hydrogenated polybutadiene) with diblock copolymers of polyethylene-poly(ethylene-*alt*-propylene), E/EP, varying both homopolymer loading and the block copolymer and homopolymer molecular weights. The pure block copolymers form homogeneous melts which are miscible with the homopolymer. The two components readily cocrystallize, even at homopolymer loadings as high as 75 wt % and even for a homopolymer which has nearly three times the molecular weight of the E block in the diblock. Small-angle X-ray scattering (SAXS) shows a single domain structure up to at least 50 wt % homopolymer addition, a result confirmed by transmission electron microscopy (TEM). Surprisingly, the Bragg spacing observed by SAXS, which reflects the sum of E and EP lamellar thicknesses, decreases continuously and substantially as homopolymer is added. The strong chain stretching in the EP block is progressively relaxed as E homopolymer is added; the reduction in Bragg spacing is only weakly opposed by the enthalpic resistance to formation of additional internal interface between E and EP domains, due to the small interaction parameter between the two blocks.

I. Introduction

Since block copolymers were first commercialized as thermoplastic elastomers, they have been blended with one or more homopolymers to tailor solid-state properties or melt processability, or to reduce costs.[1] Such systems, where all constituents are completely amorphous, have been examined in detail both experimentally[2−13] and theoretically;[14−16] a representative example is a styrene−diene block copolymer blended with homopolystyrene. The broad conclusion of these investigations is that homopolymer A has substantial solubility in an AB diblock provided that its molecular weight is lower than that of the A block of the diblock. If the homopolymer (C) is miscible with but not chemically identical to one of the blocks (A) in the diblock, then solubilization of C within the A domains is either favored[4] or disfavored[13] depending on whether the Flory−Huggins interaction parameter χ between A and C is negative or positive, respectively. Limited solubility of homopolymer within the block copolymer mesophase can manifest itself in loss of the block copolymer's long-range order[12] or even in macrophase separation.[2,5,11]

In this work, we investigate blends of semicrystalline block copolymers with semicrystalline homopolymers. We have previously published morphological investigations[17−19] of unblended semicrystalline block copolymers containing a polyethylene block, prepared by hydrogenating high-1,4 polybutadiene. The other block is an amorphous polyolefin, such as poly(ethylene-*alt*-propylene), denoted EP, prepared by hydrogenating high-1,4 polyisoprene. These semicrystalline diblocks differ from their amorphous counterparts in several significant ways. First, for polymers crystallizing from single-phase melts, the morphology is lamellar[17] for as little as 12 wt % polyethylene (E) block, whereas amorphous block copolymers of the same composition would generally form spheres. Second, when the polymers crystallize from a melt mesophase,[19] the Bragg spacing can increase by as much as 50%, reflecting substantial chain stretching in the amorphous block induced by crystallization of the E block. This chain stretching was previously predicted theoretically.[20,21] While amorphous block copolymers also exhibit stretching of the chains as the segregation strength is increased,[22] such as by changing the temperature, this stretching is gradual, while in the semicrystalline systems it occurs abruptly upon crystallization.

While the mechanical properties for polyethylene-based block copolymers blended with polyethylene or polypropylene have been described,[23] there do not appear to be any reports of morphology. Many of these blends are likely to show macrophase separation between homopolymer and block copolymer, due either to immisicibility in the melt between polyolefins of different chemical structure,[24,25] or to phase separation upon crystallization due to differences in crystallization temperature between the homopolymer and the crystallizable block.[26−28] Here, we investigate the solubility of E homopolymer within the E domains of E/EP diblocks. (Although the E "homopolymers" and the E blocks of the diblocks are structurally equivalent to statistical copolymers of ethylene with a small amount of 1-butene, we use the term "homopolymer" to more clearly distinguish the "homopolymer" and block copolymer constituents of the blends.) We examine the morphological consequences of E addition to the E/EP microdomain structure and interpret the results in the context of the substantial chain stretching present in the EP block in the absence of E homopolymer.

II. Experimental Section

Selected molecular characteristics for the polymers used in this work are given in Table 1. In the sample code, "E" indicates a hydrogenated polybutadiene homopolymer, fol-

* To whom correspondence should be addressed.
[†] Present address: Exxon Chemical Company, P.O. Box 536, Linden, NJ 07036.
[‡] Present address: Princeton Materials Institute, Princeton University, Princeton, NJ 08544.
[⊗] Abstract published in *Advance ACS Abstracts,* January 15, 1997.

S0024-9297(96)00308-7 CCC: $14.00

Table 1. Molecular and Thermal Characteristics of Blend Constituents

polymer	M_w (kg/mol)[a]	M_w/M_n[a]	f	branch content[b]	peak T_m (°C)	ΔH_f (J/g)
E/EP 7/15	21.7	1.04	0.30	20	109	37
E/EP 19/30	48.8	1.06	0.38	14	107	53
E5	5.5	1.07	1	24	115	113
E19	19.0	1.03	1	19	116	135

[a] For diblocks, values refer to entire polymer. [b] Ethyl branches per 1000 backbone carbon atoms in E block or E homopolymer.

lowed by digits which indicate the approximate molecular weight (in kg/mol); "E/EP" indicates a hydrogenated butadiene/isoprene diblock, with the approximate molecular weights of the E and EP blocks given by the digits. Synthesis and characterization of the E/EP 7/15[18] and E/EP 19/30[17] have been described previously. Briefly, the 1,4-butadiene/1,4-isoprene precursors to the E/EP diblocks were synthesized by high-vacuum anionic polymerization,[29] using *tert*-butyllithium as initiator, with the butadiene block synthesized first. Size exclusion chromatography (SEC) showed the diblocks to be free from any products of premature termination and provided the values of M_w/M_n listed in Table 1. Molecular weights of the precursor diblocks were obtained by low-angle laser light scattering and compositions from ^{1}H nuclear magnetic resonance (NMR). Compositions are expressed as the weight fraction of E block, denoted f. ^{1}H NMR also provided the microstructure of the polybutadiene block (5−9% 1,2 addition). These 1,2 units become ethyl branches upon saturation; Table 1 lists the branch content of the E blocks in each polymer calculated from the microstructure of the polybutadiene precursor. The isoprene microstructure was typically 94% 1,4 and 6% 3,4 addition. The precursors to E5 and E19 were anionically-synthesized high 1,4 polybutadienes. The precursor to E19 was graciously provided by Mr. J. A. Sissano of Exxon Research and Engineering, while the precursor to E5 was an SEC standard polybutadiene (CDS-B-7) purchased from Goodyear Tire & Rubber Company. Molecular weight and microstructure for the E19 precursor were determined by SEC and ^{1}H NMR at Princeton;[30] the corresponding values for the E5 precursor were provided by Goodyear (from light scattering and ^{1}H NMR). The precursors to E5 and E19 were saturated with H_2 over a $Pd/BaSO_4$ catalyst, as described previously.[17,18,31] Previous high-temperature SEC measurements[17] on E homopolymers and E/EP diblocks hydrogenated in this manner have shown that no chain scission or branching occurs during hydrogenation.

Three blend series were prepared, with varying component ratios: E19 with E/EP 7/15, E19 with E/EP 19/30, and E5 with E/EP 7/15. Blends of the polymers were prepared by co-dissolution of the polymers at approximately 1 wt % in heptane at 90 °C. A large quantity (40 volumes per volume heptane) of an acetone/methanol mixture (roughly 50/50 v/v) at room temperature was poured into the hot heptane solution with vigorous stirring. Precipitated polymer was collected on an Anodisc filter (0.22 μm) and then dried in a vacuum oven at room temperature. The recovered blend powders were melted at 150 °C under vacuum in polytetrafluoroethylene dishes and allowed to flow under their own weight into films. The oven temperature was lowered to 75−80 °C, and the samples were annealed for 24−36 h to emulate the thermal treatment used in our previous work.[17] Films of the pure components were prepared analogously. Blend compositions are denoted by the parameter w_E, the weight fraction of E homopolymer in the blend (*e.g.*, $w_E = 0.75$ represents a 3:1 w/w ratio of homopolymer to diblock).

Differential scanning calorimetry (DSC) was performed on a Perkin-Elmer DSC-7 calibrated with indium and mercury. Samples were initially quenched to −20 °C, then heated to 150 °C at 10 °C/min ("first heat"), and then cooled to −20 °C at 10 °C/min ("cool"). Values of the peak melting temperature (T_m) and the total enthalpy of fusion (ΔH_f) for the pure components on the first heat are given in Table 1. To within experimental error, the enthalpies of crystallization measured on cooling (ΔH_c) were identical to ΔH_f. Small-angle X-ray scattering (SAXS) measurements employed a compact Kratky camera and Braun position-sensitive detector. Data were collected, reduced, and smoothed using previously reported procedures[32] and expressed as the desmeared absolute intensity I/I_eV vs the scattering vector $q = (4\pi/\lambda) \sin \theta$, where λ is the radiation (Cu Kα) wavelength and 2θ is the scattering angle. Background intensities were determined as the average value of the scattered intensity at high q ($\approx$2 nm^{-1}) and were subtracted from the data. Intensities are multiplied by q^2 in anticipation of a lamellar morphology,[33] as has been found previously for the pure components.[17,18] Specimens for transmission electron microscopy (TEM) were prepared by gluing a small block of material onto an applicator stick, microtoming a flat face onto the block, and then staining for 3−5 h by immersion into aqueous 0.5% RuO_4. The stained sample faces were carefully trimmed to remove the heavily stained crust and then cryosectioned at −130 °C using a Reichert-Jung FC-4D microtome equipped with a Diatome 45° diamond knife. Stained sections approximately 70 nm thick were collected on copper grids and examined in bright field at 160 kV using a JEOL 2000FX; images were recorded on Kodak SO163 film. Magnification calibration for the TEM employed a diffraction grating with a 2160 lines/mm pitch. All TEM work was performed at Exxon Chemical, Baytown Polymers Center.

III. Results

A. Blend Miscibility. Both experiment[2,5,11] and theory[14,16] indicate that the miscibility of amorphous block copolymers with homopolymers is limited, even when the homopolymer is chemically identical to one of the blocks. The formation of a separate phase of pure homopolymer is favored when the loading of homopolymer is large and/or when the molecular weight of the homopolymer exceeds the molecular weight of the corresponding block. Therefore, the most basic question to ask for our semicrystalline block copolymer/semicrystalline homopolymer blends is whether they are fully miscible. Immiscibility could arise from two sources: immiscibility in the melt or segregation of components during crystallization. From small-angle neutron scattering on blends of E and EP homopolymers in the melt,[34,35] the Flory−Huggins interaction parameter χ over the range 391−440 K is well represented by

$$\chi(T) \times 10^3 = -15.9 + 8760/T(\mathrm{K}) \qquad (1)$$

where the reference volume is the geometric mean of the monomer volumes at the specifed temperature (monomer volumes correspond to 56.10 g/mol for E and 70.13 g/mol for EP). We have previously shown[17,18] that the two E/EP diblocks studied here form homogeneous melts (*i.e.*, not microphase separated). Whether a homogeneous diblock and a homopolymer should show melt miscibility or not can be roughly estimated by assuming that the homogeneous diblock has a cohesive energy density (square of the solubility parameter) which is the weighted average of those of the two blocks. The solubility parameter approach has been shown to give an adequate representation of the χ parameters for many polyolefins,[24,25] including E and EP. Neglecting the small differences in reference volume and density, this approach produces a rescaled χ_{eff} between the diblock and the homopolymer:

$$\chi_{eff} = (1 - f)^2\chi \qquad (2)$$

where f is the volume fraction of the diblock comprised by the block chemically identical to the homopolymer (here, E). Because of the minuscule differences in density between E and EP in the melt,[17] weight and volume fractions can be used interchangeably for f. The

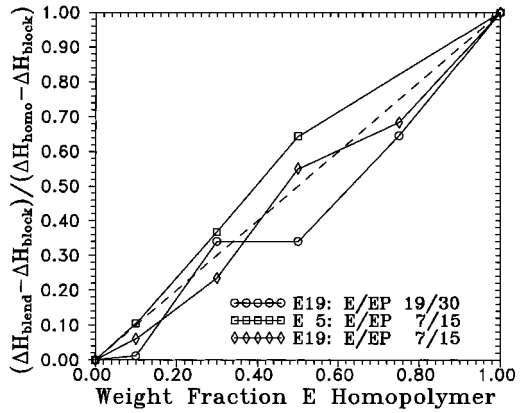

Figure 1. Normalized enthalpies of fusion ΔH for all three blend series. The subscripts "blend", "block", and "homo" refer to the enthalpies of the blend and its pure block copolymer and homopolymer constituents, respectively. Dashed diagonal depicts a simple mass-weighted average of the enthalpies of the blend constituents and represents the data to within experimental error: (○) E19:E/EP 19/30 blend series, (□) E5: E/EP 7/15 blend series, (◊) E19:E/EP 7/15 blend series.

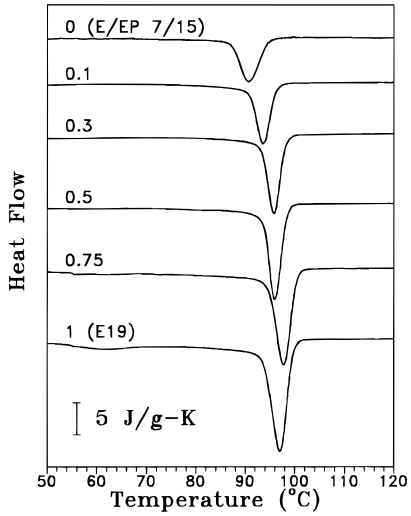

Figure 2. DSC cooling cooling scans (10 °C/min) for the E19: E/EP 7/15 blend series. Numbers adjacent to each curve indicate the weight fraction of E19 (w_E) in each blend. Note the narrow monomodal exotherm observed in all cases.

blend system having the highest molecular weight, and thus the greatest tendency toward immiscibility, is E19 blended with E/EP 19/30; in this case, the product $\chi_{eff}N \approx 1.2$ for a 50/50 w/w blend at 120 °C, where N is the average degree of polymerization. Since this lies below the critical value of 2 for immiscibility, we expect all our blends to show single-phase melts.

A more likely source of immiscibility is separate crystallization of the components on cooling. Several studies of binary polyethylene blends have shown that slight differences in melting point, due to variations in either molecular weight[26] or chain branching,[27,28] can easily produce segregation of the components into separate crystalline lamellae. As Table 1 shows, the diblocks do indeed show slightly lower melting points (by 6−9 °C) than the E homopolymers. Because of the fairly broad melting ranges of these polymers,[17,27,28] the DSC heating curves for the pure components overlap severely and, thus, do not provide useful information on whether the blend components cocrystallize or not. As shown in Figure 1, the enthalpies of fusion of the blends are consistent with a weighted average of the enthalpies of the blend components (dashed line), within experimental error; the large scatter in the data arises from the long, low-temperature tail of the DSC curves.[17,27,28] However, regardless of whether the polymers are crystallizing together or separately, the enthalpy of fusion of the blends should approximately follow the dashed line in Figure 1.

By contrast, the DSC cooling curves were found to provide valuable information[28] on the presence of cocrystallization because the primary crystallization exotherm is rather narrow. Moreover, the peak temperature of the exotherm varies by 12 °C among the blend components. Examples of DSC cooling curves are given in Figure 2, for the E19:E/EP 7/15 blend series. In this series the E homopolymer has nearly three times the molecular weight of the E block in the diblock; yet in all cases the primary crystallization exotherm is monomodal and narrow, with a full width at half-maximum (FWHM) of roughly 4 °C. The results for the other two blend series are qualitatively similar; Table 2 lists the measured values of the peak crystallization temperatures (T_c) and breadths for all of the blends examined. The narrow peak widths observed in all cases (comparable to those of the pure components), coupled with the substantial separation in peak temperatures for the pure components, indicate that these polymers freely cocrystallize on cooling at 10 °C/min. These results also confirm our expectation that these polymers are fully miscible in the melt, as melt immiscibility would also result in separate crystallization of the components. Inspection of Table 2 shows that the exotherm peak temperatures for the blends do *not* follow a weighted average of the pure-component values, but rather are heavily skewed toward the value corresponding to the component with the higher T_c. Thus, blends which contain only 30% E homopolymer have crystallization temperatures within 2 °C of the pure E homopolymer. These results suggest a mechanism where the initiation of crystallization is controlled by the component with the higher T_c, but once crystallization commences, the two components cocrystallize freely.

Table 2. Thermal and Morphological Characteristics of Blends

blend series	w_E	peak T_c (°C)	peak breadth (°C)[a]	q^* (nm^{-1})	σ_j (nm^2)
E19:E/EP 7/15	0	91	4.3	0.162	2.14
	0.1	94	3.4	0.166	2.42
	0.3	96	3.1	0.176	3.27
	0.5	96	4.3	0.185	4.77
	0.75	98	3.4	0.24[b]	
	1	97	3.5	0.47[c]	
E19:E/EP 19/30	0	89	3.8	0.113	2.97
	0.1	92	3.9	0.127	3.69
	0.3	98	3.8	0.140	5.18
	0.5	97	3.2	0.152	7.81
	0.75	97	3.7	0.19[b]	
	1	97	3.5	0.47[c]	
E5:E/EP 7/15	0	91	4.3	0.162	2.14
	0.1	95	6.8	0.164	2.39
	0.3	99	6.2	0.190	3.53
	0.5	98	4.5	0.225	5.80
	1	101	5.2	0.36[c]	

[a] Full width at half-maximum of the primary crystallization exotherm. [b] Lamellar structure significantly less regular than in blends with lower w_E. [c] Corresponds to d', not d.

B. Blend Morphology. Having established that these blends readily cocrystallize, we proceeded to investigate their morphology by small-angle X-ray scattering (SAXS), under the premise that the scattering patterns would reflect a single structure rather than the two structures expected in a macrophase-separated

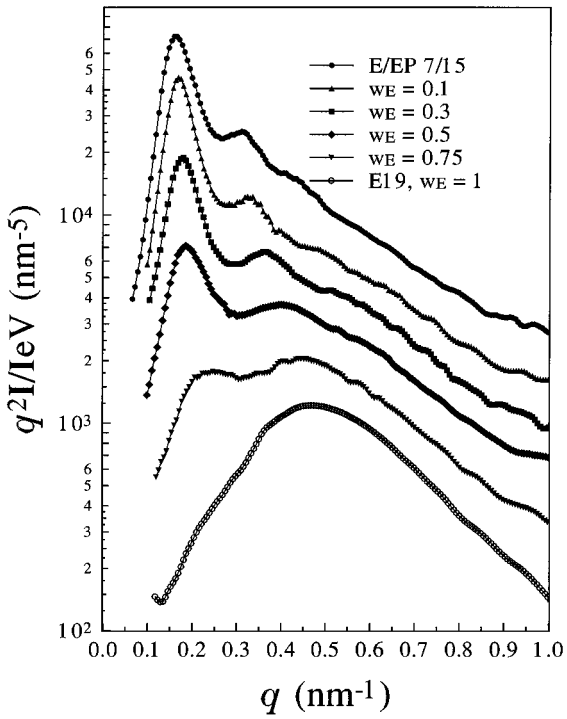

Figure 3. q^2-corrected SAXS data for the E19:E/EP 7/15 blend series. For clarity, the intensities for each curve have been multiplied by a scale factor, given in square brackets: (●) w_E = 0 [4.0]; (▲) w_E = 0.1 [2.4]; (■) w_E = 0.3 [1.0]; (◆) w_E = 0.5 [0.32]; (▼) w_E = 0.75 [0.16]; (○) w_E = 1 [0.080].

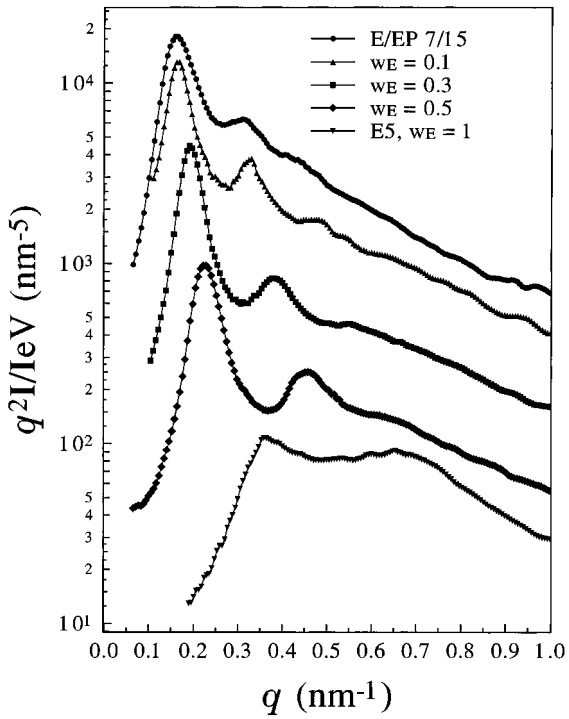

Figure 4. q^2-corrected SAXS data for the E5:E/EP 7/15 blend series. For clarity, the intensities for each curve have been multiplied by a scale factor, given in square brackets: (●) w_E = 0 [1.0]; (▲) w_E = 0.1 [0.50]; (■) w_E = 0.3 [0.11]; (◆) w_E = 0.5 [0.032]; (▼) w_E = 1 [0.017].

blend.[28] As discussed previously,[17,18] the pure E/EP 7/15 and E/EP 19/30 diblocks show an alternating lamellar morphology with a high degree of order, as evidenced by 2−3 SAXS reflections in a q ratio of 1:2(:3). The overall Bragg spacing d in the diblocks corresponds to the sum of E and EP domain thicknesses; d is obtained from the position of the first-order maximum q^* by

$$d = 2\pi/q^* \tag{3}$$

By contrast, hydrogenated polybutadiene homopolymers generally show only a single broad peak[17,18] near q^* = 0.5 nm^{-1}, corresponding to the sum of the thicknesses of the E crystallites and the interlamellar amorphous regions, which we have previously denoted d'. This same structure presumably exists within the E domains in the block copolymer, for sufficiently long E blocks, and indeed this has been demonstrated by SAXS[17] for some E/EP diblocks.

Figure 3 shows SAXS data for the E19:E/EP 7/15 series, corresponding to the DSC traces in Figure 2. The morphology clearly remains lamellar up to a homopolymer content of 30%, as indicated by the persistence of two narrow SAXS reflections in a q ratio of 1:2, as well as a weak third-order reflection. At 75% homopolymer addition, two reflections are still evident (at 0.25 and 0.46 nm^{-1}), but the intensity and breadth of the higher q reflection suggests that it arises from the d' spacing (internal to the E domains, and exhibited by both the pure block copolymer and homopolymer)[17,19,36] and is not directly related to the peak at 0.25 nm^{-1}. Moreover, the increased breadth of the low-q peak relative to blends with lower E content suggests increased disorder in this blend. The blend with 50% homopolymer represents an intermediate case; two peaks are observed, but the second-order peak is much broader than at lower homopolymer loadings and occurs at 2.15 times the q value of the first-order peak. Thus, the observed second-order peak may represent a superposition of a true second-order peak and the scattering due to d'. Note that the EP volume fraction in the blend with w_E = 0.50 is approximately 0.36, and in the blend with w_E = 0.75, it is only 0.18. It is quite possible that the EP domains cease to be "continuous" at very high homopolymer loadings; that is, rather than forming lamellae of very large lateral extent, the EP phase is broken up into unconnected domains of limited lateral extent. Our previous results[17] demonstrating a lamellar morphology in pure E/EP diblocks extended only down to EP volume fractions of 0.47, so the morphology at lower EP volume fractions is unknown. Note that as the level of E19 in the blends increases, the value of q^* increases, meaning that the Bragg spacing d decreases. This unexpected result, which was found for all three blend series, will be addressed in detail in the Discussion.

The results for the other two blend series are shown in Figures 4 and 5 and are qualitatively similar to those for E19:E/EP 7/15. Values of q^* for all blends and pure components are given in Table 2. A few small but significant differences should be noted between the three blend series. First, the SAXS pattern for the pure E5 differs substantially from that for E19, consisting of a narrow primary peak at 0.36 nm^{-1} and a broader second-order reflection at 0.7 nm^{-1}. Since the ethyl branch content of E5 is actually *higher* than that of E19, this indicates that the lower molecular weight of E5 is the cause of the longer stem lengths and more uniform spacings, even though the Bragg spacing of E5 corresponds to only about one-third of the calculated length of an extended-chain crystal. A similar increase in Bragg spacing and regularity has been reported previously[28] for a hydrogenated polybutadiene of even lower molecular weight (3.8 kg/mol). By contrast, hydrogenated polybutadienes of molecular weights higher than E19 show essentially the same SAXS pattern[17,18] as E19. Second, by comparing Figures 3 and 4 at w_E = 0.5, it

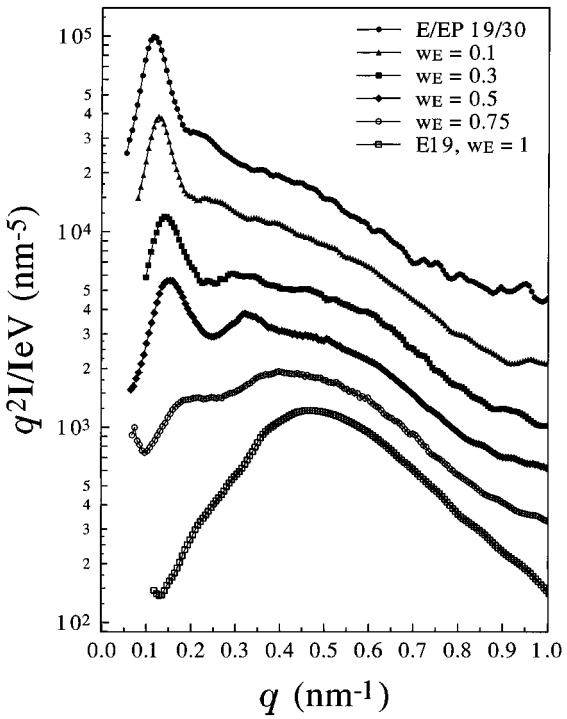

Figure 5. q^2-corrected SAXS data for the E19:E/EP 19/30 blend series. For clarity, the intensities for each curve have been multiplied by a scale factor, given in square brackets: (●) $w_E = 0$ [3.8]; (▲) $w_E = 0.1$ [3.0]; (■) $w_E = 0.3$ [1.0]; (◆) $w_E = 0.5$ [0.35]; (○) $w_E = 0.75$ [0.17]; (□) $w_E = 1$ [0.080].

becomes evident that the longer homopolymer creates somewhat more disorder in the microdomain structure than the shorter homopolymer. Indeed, a weak third-order reflection can still be seen in the E5:E/EP 7/15 blend with $w_E = 0.5$, while for the analogous E19:E/EP 7/15 blend the second-order reflection is already weak. A similar comparison can be made between Figures 3 and 5, again focusing on the $w_E = 0.5$ blends: when the molecular weight of the E homopolymer far exceeds that of the E block in the diblock (E19:E/EP 7/15), the regularity of the domain spacings is diminished (vs E19: E/EP 19/30).

To confirm the morphological assignments given above, and to obtain more insight into the morphology of the $w_E = 0.75$ specimens, TEM was performed on selected members of the E19:E/EP 19/30 blend series. Contrast in these specimens was achieved by preferential diffusion of RuO_4 into amorphous regions, which appear black in the positive images shown in Figure 6. Beginning with the pure E/EP 19/30 ($w_{E19} = 0$), a lamellar structure is clearly evident, with bright E domains and dark EP domains possessing a rather regular domain spacing. In the blend with $w_{E19} = 0.5$, the same general morphology is presented, but with a somewhat reduced spacing. Moreover, the relative widths of the light and dark stripes (corresponding to E and EP, respectively) increases over the pure E/EP 19/30, as expected given the substantial addition of E homopolymer. Finally, in the blend with $w_{E19} = 0.75$, the majority of the sample appears to consist of a lamellar structure similar to that exhibited by the $w_{E19} = 0$ and $w_{E19} = 0.5$ materials, although with a further-reduced interlamellar spacing and a very high ratio of light to dark (E to EP) in the image. However, near the top of the image shown, the degree of order of the lamellar structure is considerably reduced, and and it appears that isolated dark regions (microdomains of EP) are present. Thus the TEM results shown here are in complete agreement with the SAXS results discussed above, and show that at very high E contents (around $w_{E19} = 0.75$ here, or 85% total E), continuity of the EP domains is disrupted. Due to the greater irregularity in the morphology of the blend with 75% E19, the Discussion will focus on blends containing 50% homopolymer or less.

For comparison, a TEM image of the pure E19 homopolymer ($w_{E19} = 1$) is shown in Figure 6 as well. The contrast in this image is considerably less than in the pure diblock or blends, presumably because the RuO_4 cannot diffuse as readily into the thin intercrystallite spaces in E19 as it can into the relatively thick EP domains in the pure diblock or blends. Relatively thin crystals are visible in this image; in some cases, gray stripes are evident between the brighter white stripes. These gray stripes presumably reflect thin crystals which may have been partially attacked by the stain. On the basis of our previous work[17−19] and the SAXS results discussed above, we infer that the structure present in the E19 specimen is also present within the E domains (white stripes) evident in the TEM images of the pure diblock and blends. However, given the limited contrast between crystalline and amorphous E evident in the TEM image of E19, compared with the greater contrast between E and EP evident in the pure diblock and blend images, it is perhaps not surprising that the internal structure of the E domains is not apparent. The inability of TEM to resolve the crystallite structure within the microdomains of polyethylene-containing block copolymers has been reported previously.[37] It is also worth noting that lower magnification TEM images (not shown) indicate that the lamellar stacks evident in Figure 6 are part of the sheaflike structures which comprise spherulites. We have previously shown that the pure E/EP diblock and E homopolymer both form spherulites of similar size, so it is not surprising that the blends do so as well.

Finally, Table 3 lists repeat distances for the E19:E/EP 19/30 blend series, obtained by both SAXS and TEM. The values for the TEM images were derived by manual measurement of the widths of several lamellar stacks for each image. For E19, only regions of the image with good contrast (such that the gray stripes mentioned above were distinguishable) were considered in the averaging. Note that for the pure E19, the spacing derived corresponds to d', while for the other materials it corresponds to d. The d values obtained by both methods show the interdomain spacing decreasing considerably as the homopolymer content increases. However, the values obtained from the TEM images are all 15−25% lower than the values from SAXS. Since the SAXS measurements do not require any staining or microtoming, we feel that the d values obtained by SAXS are more reliable. The advantage of complementary TEM examination, as presented here, is to confirm the morphological conclusions reached from the SAXS data, as well as providing additional information on more poorly ordered specimens such as that with $w_{E19} = 0.75$.

IV. Discussion

Considered in the context of the literature on amorphous diblocks blended with homopolymers, our results are surprising on two counts. The first is that the blends show only a single structure (no macrophase separation) up to an E homopolymer weight fraction w_E of at least 0.50. This is true even when the homopoly-

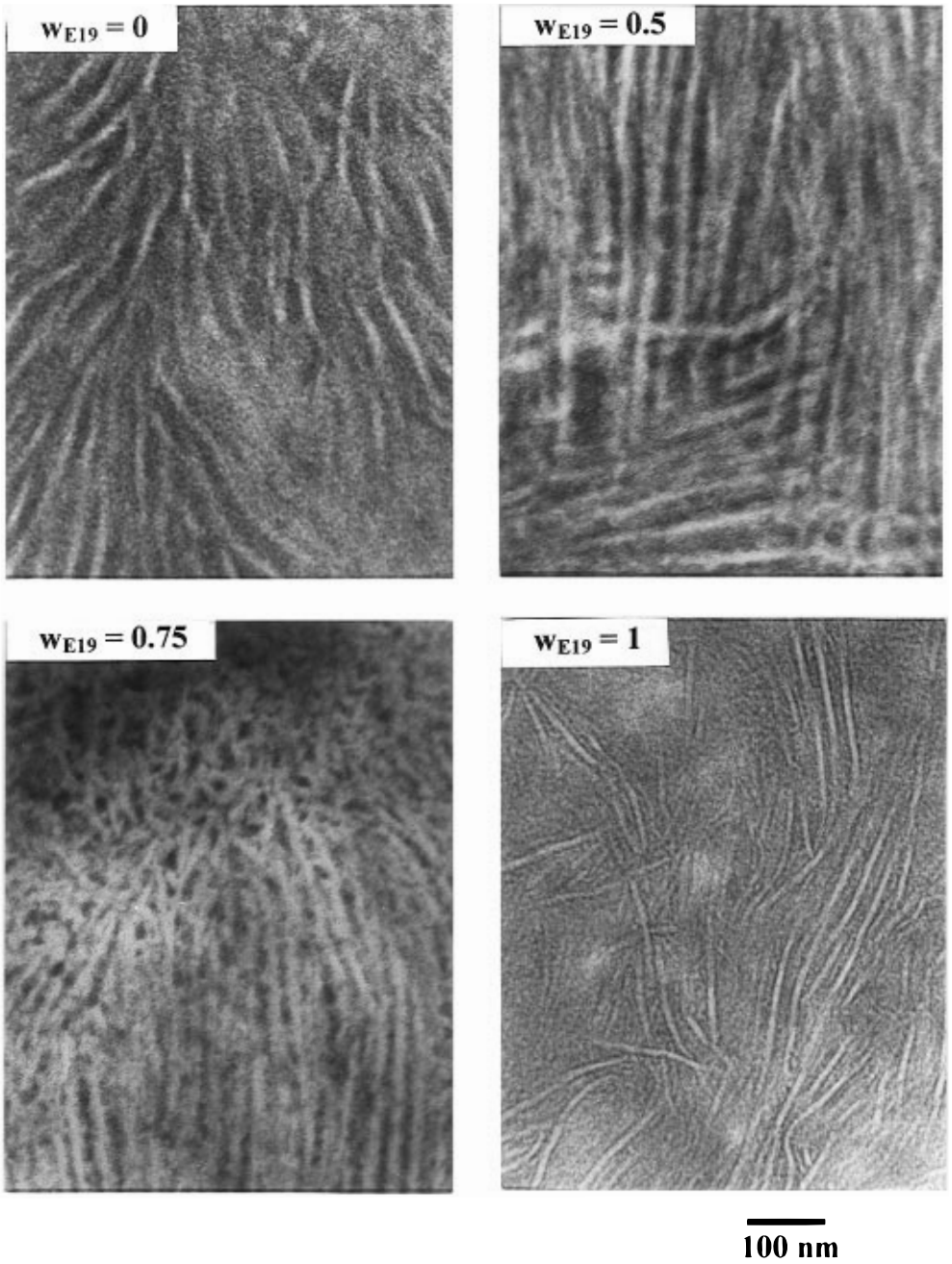

Figure 6. Bright-field TEM images of RuO_4-stained specimens of four members of the E19:E/EP 19/30 blend series. Top left to bottom right: $w_{E19} = 0$ (pure E/EP 19/30), $w_{E19} = 0.5$, $w_{E19} = 0.75$, and $w_{E19} = 1$ (pure E19).

Table 3. Interdomain Spacings *d* for the E19:E/EP 19/30 Blend Series

	d (nm)	
w_{E19}	from TEM	from SAXS
0	41	55.6
0.5	33	41.3
0.75	28	33.1
1	11[a]	13.4[a]

[a] Corresponds to *d′*, not *d*.

mer has nearly three times the molecular weight of the corresponding block. The second surprising result is that the Bragg spacing decreases continuously as the homopolymer content increases, up to at least $w_E = 0.50$, and represents as much as a 28% contraction (E5:E/EP 7/15, $w_E = 0.50$) relative to the pure diblock.

The first of these points has been addressed both theoretically and experimentally for purely amorphous systems. Whitmore and Noolandi[14] calculated that the solubility of amorphous homopolymer in the mesophase of an amorphous diblock should decrease rapidly once the homopolymer's molecular weight exceeds that of the corresponding block. Quan *et al.*[2,11] found experimentally that when polybutene homopolymer is added to a lamellar styrene−butene−styrene triblock, almost all of the homopolymer is excluded into separate domains when its molecular weight exceeds that of the corresponding midblock. Cheng *et al.*[5] also reported the segregation of homopolybutadiene from a styrene−butadiene diblock containing spherical domains of polybutadiene, with a separate homopolymer phase appearing at lower loadings for higher molecular weights, indicating that the phenomenon is not exclusive to the triblock architecture or the lamellar morphology. More recently, Koizumi *et al.*[12] studied a styrene−isoprene diblock blended with styrene homopolymer of similar

molecular weight to the styrene block. Although macrophase separation was not observed even at high homopolymer addition, the long-range order of the lamellar structure was adversely affected by the added homopolymer; while the pure diblock showed at least 10 SAXS reflections corresponding to the repeat distance of the styrene−isoprene domains, a blend containing 60% polystyrene homopolymer showed *no* Bragg peaks, only broad maxima characteristic of the isolated isoprene lamellae. This "unbinding transition" has recently been found in a theory by Matsen,[16] and is predicted to occur only when the homopolymer corresponds to the majority component of the diblock. Thus, in all cases, attempts to add large concentrations of high molecular weight amorphous homopolymer to an amorphous diblock result in either macrophase separation or severe loss of long-range microdomain order, in contrast to our observations on semicrystalline systems.

The effect of homopolymer on the Bragg spacing, the source of our second surprising result, has also received much attention in amorphous systems. Hashimoto *et al.*[6] and Winey *et al.*[7] performed detailed studies of lamellar blends of a styrene−isoprene diblock with polystyrene homopolymers. In general, the Bragg spacing increased with homopolymer addition, and the rate of increase was greater the larger the homopolymer molecular weight. Under the simplistic assumption that the B layer in a blend of AB diblock with A homopolymer retains a constant thickness as homopolymer is added, one would expect a monotonic increase in Bragg spacing with homopolymer addition, at a rate which is independent of molecular weight. By contrast, Winey *et al.*[7] found that for homopolymers having a molecular weight less than the corresponding block, blends with low loadings of homopolymer actually had *smaller* Bragg spacings than the pure diblock. This observation was explained by considering the substantial chain stretching present in the pure diblocks, and how the extent of stretching can be reduced by the addition of homopolymer.[7,15] However, the magnitude of the Bragg spacing contraction was never very large—less than 4% in the published data[7]—and the minimum in Bragg spacing was reached at rather low homopolymer loadings, only about 10% even for a homopolymer with only 1/10 the molecular weight of the corresponding block. These observations contrast sharply with ours, where a Bragg spacing contraction is observed even on adding high molecular weight homopolymer, and where the magnitude of the contraction is large (up to 28%). Since we observe the contraction for blends with homopolymer loadings up to 50%, a minimum in the Bragg spacing, if one exists, must occur at even higher homopolymer loadings. Thus, we find substantial qualitative and quantitative differences between our crystallizable systems and the amorphous systems studied to date.

The reduction in Bragg spacing upon the addition of homopolymer can be related to the large degree of stretching induced in the amorphous block upon crystallization of the other block, to which it is attached.[20,21] The Bragg spacing d, as defined in eq 3, is the sum of the crystalline and amorphous domain widths. Because the two blocks are covalently bound together, and because the microdomains possess essentially the same densities as their homopolymers, if the crystallizable layer in a lamellar structure thickens upon crystallization, then the amorphous layer must thicken as well. This thickening of the amorphous layer necessarily leads to a proportional degree of stretching of the amorphous chains. In a few cases, this stretching has been observed directly, by comparing the Bragg spacing for a lamellar block copolymer in a melt mesophase and in the semicrystalline state. Nojima *et al.*[38] found an 80% increase in Bragg spacing upon crystallization of a caprolactone−butadiene diblock having a lamellar mesophase. Similar observations have been reported by Ryan *et al.*[36] (40% increase for an ethylene−butene diblock), Rangarajan *et al.*[19] (50% increase for an ethylene−(head-to-head propylene) diblock, slow-cooled and annealed), and Yang *et al.*[39] (140% increase for an oxyethylene−oxybutylene diblock, comparing the spacing for the crystallized sample with the spacing corresponding to the correlation hole peak observed in the homogeneous melt).

As mentioned above, both E/EP diblocks studied here as well as the many others studied in our previous work[17,18,35] are all homogeneous in the melt. Moreover, the electron density contrast between E and EP is minuscule—they have the same empirical formula and identical mass densities[17] to roughly one part in 10^3—and thus the correlation hole peak is not observable in any of our materials, even with a synchrotron X-ray source.[18] However, an estimate of the degree of chain stretching can still be obtained by calculating the q^* value of the correlation hole peak, using mean-field theory[40,41] and the known segmental characteristics of the blocks[42] at 140 °C. These calculations were performed for a range of E/EP diblocks which we have previously characterized,[35] having $0.15 < f < 0.56$ and total molecular weights ranging from 11 to 117 kg/mol. The ratio of the Bragg spacing of the crystallized material at 23 °C to the spacing corresponding to the calculated correlation hole peak at 140 °C was 1.95 ± 0.19, with no apparent trends with composition or molecular weight. Note that this comparison neglects the increase in density which accompanies crystallization, as well as changes in the segmental characteristics between 140 and 23 °C; however, these effects are much smaller than the 95% increase in Bragg spacing produced by this rough calculation. It also neglects any possible chain stretching in the melt, which is known to occur as the order−disorder transition is approached; however, given the small values of χN (<6) which these block copolymers possess, we would expect Gaussian chain statistics to be a good approximation for our E/EP diblocks in the melt.[43] The calculated q^* values at 140 °C for E/EP 7/15 and E/EP 19/30 are 0.343 and 0.221 nm^{-1}, respectively, which may be compared with the observed q^* values for the crystallized polymers of 0.162 and 0.113 nm^{-1}, respectively.

These observations and calculations demonstrate that the EP blocks in our pure E/EP diblocks are highly stretched, and this certainly provides a driving force for the solubilization of E homopolymer and the consequent reduction in Bragg spacing. However, amorphous block copolymers can also exhibit strong chain stretching when the segregation strength is sufficiently large. Calculations analogous to those described above were performed for the styrene−isoprene diblock (SI 27/22) studied by Winey *et al.*,[7] to obtain the position of the interference maximum for the hypothetical homogeneous melt. Comparison of this calculated value with the experimentally observed Bragg spacing for the segregated diblock indicates a quantitatively similar degree of chain stretching (80%) to that found in our semicrystalline E/EP 19/30. Thus, while chain stretching is present in our E/EP diblocks, this is insufficient

to explain the differences between our observations and those on amorphous homopolymers.

The additional difference between the semicrystalline system described here and amorphous systems lies in the enthalpic cost of producing internal interface in the material, which occurs whenever the Bragg spacing is reduced. In amorphous block copolymers, which microphase separate due to incompatibility between the blocks, it is the enthalpic cost of these interfaces which drives the chains to stretch, thereby reducing the specific internal interface.[22] In amorphous block copolymers, therefore, any relaxation of the chains which the added homopolymer permits is opposed by the high cost of producing additional internal interface, thus severely limiting the magnitude of the Bragg spacing contraction. In our E/EP diblock copolymers, by contrast, the cost of producing additional E/EP interfaces is small, due to the small χ between E and EP (eq 1), which is roughly an order of magnitude lower than the χ for the styrene−isoprene pair,[44] meaning that χN for our E/EP 19/30 is an order of magnitude lower than that for the SI 27/22 studied by Winey *et al.* The minimal penalty for creating additional internal interface thus allows for the large Bragg spacing contractions we observe.

To provide for more quantitative discussion, the measured Bragg spacings were converted to specific areas per block junction σ_j for a lamellar morphology via[7]

$$\sigma_j = 2(1 - f)M_w/[N_a\rho_{EP}(1 - \phi_E)d] \qquad (4)$$

where M_w is the weight-average molecular weight of the diblock, N_a is Avogadro's number, ρ_{EP} is the mass density[45] of EP at 23 °C (0.854 g/cm^3), and ϕ_E is the volume fraction of E (E block plus E homopolymer) in the blend. (Strictly speaking, the quantity $(1 - f)M_w$ in eq 4 should be replaced by the number-average molecular weight of the EP block, a quantity which is not experimentally accessible. However, the difference is minimal for the narrow-distribution products of anionic synthesis which we are considering here. The same approximation was made in the calculation of the correlation hole peak position, so the comparisons given below are consistent.) Values for ϕ_E were calculated assuming an average density[46] of the E regions (containing both crystalline and amorphous E) of 0.910 g/cm^3. Values of σ_j are given in Table 2 and clearly show a monotonic increase as the homopolymer content is increased. We estimate the σ_j value corresponding to a "fully relaxed" EP lamella by taking the calculated q^* values for the homogeneous diblock melts at 140 °C and putting the associated values of d into eq 4. The resultant values of σ_j are 4.42 and 5.67 nm^2 for E/EP 7/15 and E/EP 19/30, respectively. Figure 7 shows a plot of the experimental σ_j values normalized by these calculated values. The ratio reaches unity at homopolymer loadings of roughly 40% for all three systems, indicating that relief of the chain stretching in the EP domain should provide a driving force for homopolymer solubilization up to at least 40% homopolymer content. The measured values of σ_j actually exceed the calculated values at 50% homopolymer loading, which is somewhat surprising. However, given the uncertainty in our estimate of the "fully relaxed" σ_j, this discrepancy is not too distressing.

Another point to note in Figure 7 is the comparison between the E19:E/EP 7/15 and E5:E/EP 7/15 blend systems. Both the high- (E19) and low-molecular weight (E5) homopolymers cause reductions of the Bragg spacing and increases in σ_j. However, for the same homopolymer loading, E5 produces a greater increase in σ_j than does E19. In this respect, our results parallel those of Winey *et al.*[7] and Hashimoto *et al.*,[6] who found that the increase in σ_j was larger for lower molecular weight homopolymers. These results were explained[7,15] by a nonuniform distribution of the homopolymer within the lamellae, with the homopolymer segment density becoming increasingly peaked at the center of the lamella as the homopolymer molecular weight increases. Enhancement of homopolymer segment density at the domain centers has been confirmed experimentally in a variety of other systems as well.[3,8,9,10,12,13] However, the homopolymers used in these prior investigations have molecular weights below or only slightly above that of the corresponding block in the block copolymer. For example, in the extensive study of Winey *et al.*,[7] the longest polystyrene homopolymer was less than 40% longer than the polystyrene block of the diblock. In our case, E19 has nearly *3 times* the molecular weight of the E block in E/EP 7/15, yet the differences in σ_j between the E19:E/EP 7/15 and E5:E/EP 7/15 blends are unexpectedly modest. Some difficulty in uniformly distributing the segments of the long E19 chains within the E microdomains is also evident in the increased disorder in blends with $w_E = 0.5$, when comparing E/EP 7/15 blended with either E19 or E5; in the extreme case, which we do not observe here, a "piling up" of homopolymer at the domain centers would lead to an "unbinding transition" and the complete loss of regular lamellar stacking.[12,16] The good regularity which we observe in E19:E/EP 7/15 with $w_E = 0.5$, relative to analogous blends of a styrene−isoprene diblock with homopolystyrene,[12] also shows that the tendency for homopolymer localization at the domain centers is much smaller for our semicrystalline system.

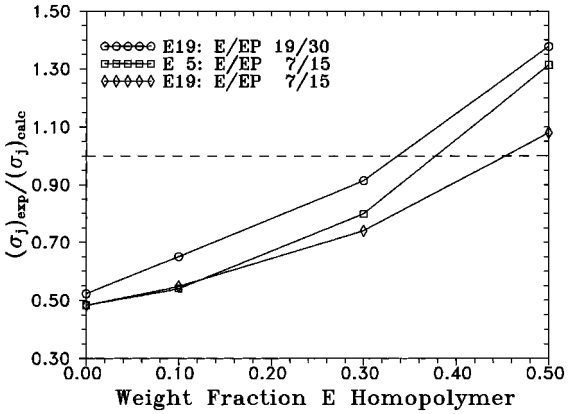

Figure 7. Normalized interfacial area per block junction for the three blend series. Dashed horizontal line represents the case where the experimental interfacial area per junction equals the area calculated for a "fully relaxed" EP lamella, as described in the text: (○) E19:E/EP 19/30 blend series, (□) E5: E/EP 7/15 blend series, (◊) E19:E/EP 7/15 blend series.

V. Conclusions

Miscibility between semicrystalline E homopolymers and semicrystalline E/EP diblocks is much greater than between amorphous homopolymers and amorphous diblocks. Cocrystallization into a single domain structure is found even for E homopolymer molecular weights nearly 3 times that of the E block in the diblock, and even for 3:1 w/w homopolymer/block copolymer ratios.

In all cases, homopolymer addition *reduces* the SAXS Bragg spacing relative to the pure diblock and increases the interfacial area per block junction. This provides relief of the chain stretching in the amorphous EP block, induced by crystallization of the E block. The large increases in interfacial area per junction contrast sharply with the much smaller increases exhibited in amorphous homopolymer/amorphous diblock systems. In the amorphous case, because the microdomain structure is created by incompatibility between the two amorphous blocks in the diblock, reductions in Bragg spacing are strongly opposed by the enthalpic cost of creating new interface between chemically different domains. In the semicrystalline case studied here, the interaction parameter between E and EP is small; microdomain formation is driven by crystallization. Thus the cost of creating new interface is small, and large Bragg spacing contractions are observed.

Acknowledgment. We thank J. A. Sissano of Exxon Research and Engineering for providing the precursor to E19, and D. J. Quiram and G. C. Reichart, both of Princeton University, for assistance in data collection. We are also most grateful to J. W. Ball and Dr. J. H. Butler of Exxon Chemical Company, Baytown Polymers Center, for performing all of the TEM work discussed herein. This work was supported by the National Science Foundation, Polymers Program (DMR-9257565), and through a summer fellowship to C. F. H. from the Princeton Center for Complex Materials, funded by the National Science Foundation MRSEC Program (DMR-9400362).

References and Notes

(1) Holden, G. In *Block and Graft Copolymerization*; Ceresa, R. J., Ed.; New York: Wiley, 1974; Vol. 1.
(2) Quan, X.; Gancarz, I.; Koberstein, J. T.; Wignall, G. D. *Macromolecules* **1987**, *20*, 1431.
(3) Berney, C. V.; Cheng, P. L.; Cohen, R. E. *Macromolecules* **1988**, *21*, 2235.
(4) Tucker, P. S.; Paul, D. R. *Macromolecules* **1988**, *21*, 2801.
(5) Cheng, P. L.; Berney, C. V.; Cohen, R. E. *Makromol. Chem.* **1989**, *190*, 589.
(6) Hashimoto, T.; Tanaka, T.; Hasegawa, H. *Macromolecules* **1990**, *23*, 4378.
(7) Winey, K. I.; Thomas, E. L.; Fetters, L. J. *Macromolecules* **1991**, *24*, 6182.
(8) Mayes, A. M.; Russell, T. P.; Satija, S. K.; Majkrzak, C. F. *Macromolecules* **1992**, *25*, 6523.
(9) Matsushita, Y.; Torikai, N.; Mogi, Y.; Noda, I.; Han, C. C. *Macromolecules* **1993**, *26*, 6346.
(10) Lee, S. H.; Koberstein, J. T.; Quan, X.; Gancarz, I.; Wignall, G. D.; Wilson, F. C. *Macromolecules* **1994**, *27*, 3199.
(11) Baetzold, J. P.; Gancarz, I.; Quan, X.; Koberstein, J. T. *Macromolecules* **1994**, *27*, 5329.
(12) Koizumi, S.; Hasegawa, H.; Hashimoto, T. *Macromolecules* **1994**, *27*, 7893.
(13) Kimishima, K.; Hashimoto, T.; Han, C. D. *Macromolecules* **1995**, *28*, 3842.
(14) Whitmore, M. D.; Noolandi, J. *Macromolecules* **1985**, *18*, 2486.
(15) Shull, K. R.; Winey, K. I. *Macromolecules* **1992**, *25*, 2637.
(16) Matsen, M. W. *Macromolecules* **1995**, *28*, 5765.
(17) Rangarajan, P.; Register, R. A.; Fetters, L. J. *Macromolecules* **1993**, *26*, 4640.
(18) Rangarajan, P.; Register, R. A.; Adamson, D. H.; Fetters, L. J.; Bras, W.; Naylor, S.; Ryan, A. J. *Macromolecules* **1995**, *28*, 1422.
(19) Rangarajan, P.; Register, R. A.; Fetters, L. J.; Bras, W.; Naylor, S.; Ryan, A. J. *Macromolecules* **1995**, *28*, 4932.
(20) DiMarzio, E. A.; Guttman, C. M.; Hoffman, J. D. *Macromolecules* **1980**, *13*, 1194.
(21) Whitmore, M. D.; Noolandi, J. *Macromolecules* **1988**, *21*, 1482.
(22) Helfand, E. *Macromolecules* **1976**, *9*, 879.
(23) Halasa, A. F. *Rubber Chem. Technol.* **1981**, *54*, 627.
(24) Graessley, W. W.; Krishnamoorti, R.; Balsara, N. P.; Butera, R. J.; Fetters, L. J.; Lohse, D. J.; Schulz, D. N.; Sissano, J. A. *Macromolecules* **1994**, *27*, 3896.
(25) Graessley, W. W.; Krishnamoorti, R.; Balsara, N. P.; Fetters, L. J.; Lohse, D. J.; Schulz, D. N.; Sissano, J. A. *Macromolecules* **1994**, *27*, 2574.
(26) Smith, P.; St. John Manley, R. *Macromolecules* **1979**, *12*, 483.
(27) Crist, B.; Yang, V. *Polym. Prepr. (Am. Chem. Soc. Div. Polym. Chem.)* **1993**, *34(2)*, 470.
(28) Ueda, M.; Register, R. A. *J. Macromol. Sci. - Phys.* **1996**, *B35*, 23.
(29) Morton, M.; Fetters, L. J. *Rubber Chem. Technol.* **1975**, *48*, 359.
(30) Ueda, M. M.S.E. Thesis, Princeton University, 1995.
(31) Rosedale, J. H.; Bates, F. S. *J. Am. Chem. Soc.* **1988**, *110*, 3542.
(32) Register, R. A.; Bell, T. R. *J. Polym. Sci. B: Polym. Phys.* **1992**, *30*, 569.
(33) Russell, T. P. In *Handbook on Synchrotron Radiation*; Brown, G. S., Moncton, D. E., Eds.; New York: North-Holland, 1991; Vol. 3.
(34) Reichart, G. C.; Rangarajan, P.; St. Hill, S.; Register, R. A.; Graessley, W. W.; Lohse, D. J. Unpublished data.
(35) Rangarajan, P. Ph.D. Thesis, Princeton University, 1995.
(36) Ryan, A. J.; Hamley, I. W.; Bras, W.; Bates, F. S. *Macromolecules* **1995**, *28*, 3860.
(37) Khandpur, A. K.; Macosko, C. W.; Bates, F. S. *J. Polym. Sci. B: Polym. Phys.* **1995**, *33*, 247.
(38) Nojima, S.; Kato, K.; Yamamoto, S.; Ashida, T. *Macromolecules* **1992**, *25*, 2237.
(39) Yang, Y. W.; Tanodekaew, S.; Mai, S. M.; Booth, C.; Ryan, A. J.; Bras, W.; Viras, K. *Macromolecules* **1995**, *28*, 6029.
(40) Leibler, L. *Macromolecules* **1980**, *13*, 1602.
(41) Benoît, H.; Hadziioannou, G. *Macromolecules* **1988**, *21*, 1449.
(42) Fetters, L. J.; Lohse, D. J.; Richter, D.; Witten, T. A.; Zirkel, A. *Macromolecules* **1994**, *27*, 4639.
(43) Almdal, K.; Rosedale, J. H.; Bates, F. S.; Wignall, G. D.; Fredrickson, G. H. *Phys. Rev. Lett.* **1990**, *65*, 1112.
(44) Adams, J. L.; Graessley, W. W.; Register, R. A. *Macromolecules* **1994**, *27*, 6026.
(45) Bates, F. S.; Schulz, M. F.; Rosedale, J. H.; Almdal, K. *Macromolecules* **1992**, *25*, 5547.
(46) Howard, P. R.; Crist, B. *J. Polym. Sci. B: Polym. Phys.* **1989**, *27*, 2269.

MA9603084